JOURNAL OF NATURAL PRODUCTS

pubs.acs.org/jnp

Article

Expanding the Diversity of the Cyanobacterial Dialkylresorcinol Bartoloside Family

João P. A. Reis, Sara Freitas, Tereza Procházková, and Pedro N. Leão*

Cite This: *J. Nat. Prod.* 2024, 87, 2709−2715

Read Online

ACCESS | Metrics & More | Article Recommendations | Supporting Information

ABSTRACT: The cyanobacterial dialkylresorcinol bartolosides were initially reported to feature glycosylated and halogenated moieties. Later, biosynthetic and *in vitro* studies showed that the chlorinated alkyl chains are utilized for a nucleophilic substitution with free fatty acid carboxylates from primary metabolism, generating bartoloside esters. Here, we applied a workflow based on PCR screening coupled to LC-HRESIMS and molecular network analysis with the aim of discovering additional bartoloside diversity. We report the annotation of 27 bartoloside and bartoloside ester derivatives, including the characterization of two new bartolosides, underlining the breadth of structures generated by bartoloside biosynthetic pathways. Some of the herein reported bartolosides feature hydroxylation in their side chains, a modification that has not been associated with this metabolite family.

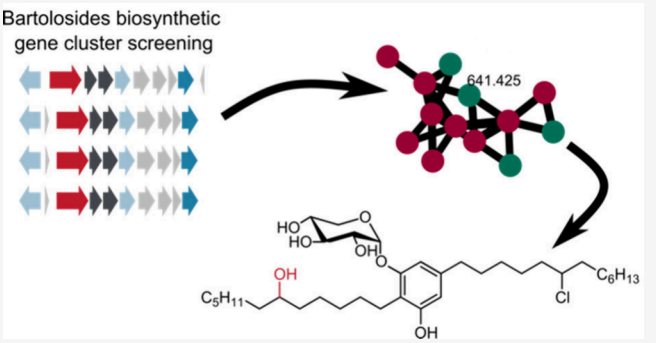

Over the past decades, cyanobacteria have emerged as one of the most promising bacterial sources of natural products, with many members of the phylum displaying biosynthetic gene cluster (BGC)-rich genomes.[1] The isolated compounds and BGC composition of these organisms indicate that their natural products space is quite differentiated from other bacterial groups.[2,3] One example of natural products unique to cyanobacteria are the bartolosides, unusual glycolipid secondary metabolites whose production is encoded by the *brt* BGC (Figure 1).[4−6] Bartolosides are dialkylresorcinols (DAR) generated via condensation (catalyzed by BrtD) of common lipid primary metabolism precursors, specifically an α,β-unsaturated fatty acyl-ACP thioester with a β-keto-fatty acyl-ACP, followed by oxidative aromatization by the FMN-dependent aromatase BrtC.[5] The bartoloside DAR skeleton is then decorated by Brt enzymes through C- and/or O-glycosylations in the aromatic ring and chlorinations in the alkyl chains.[4−6] We later reported the discovery of bartoloside-fatty acid esters, generated by the BrtB-catalyzed O-alkylation of a variety of free fatty acid carboxylates.[6] Bartolosides and their esters have been reported from three strains of the LEGE culture collection (LEGE-CC)[8] belonging to the *Synechocystis* and *Nodosilinea* genera.[4−6]

We considered that additional bartoloside diversity could be found, because (1) phylogenetically closely related strains bearing *brt* genes have not been screened for bartoloside production and (2) there is considerable promiscuity exhibited by BrtD and BrtB as to acyl chain length and composition of their respective substrates.[4−6] In addition, discovering new analogues could lead to insights into how these abundant molecules are metabolized and therefore their role in the cells. Hence, in this work, we performed a genetic (PCR) and metabolomic screening (liquid chromatography coupled to HRMS analysis and molecular networking)[7] to detect additional bartoloside-producing strains and to reveal 27 new bartoloside derivatives. Among these, we identified hydroxylation of the alkyl chain in the DAR skeleton as a novel structural feature of this metabolite family.

RESULTS AND DISCUSSION

Screening of New Bartoloside Producers. Reported bartoloside scaffolds were previously isolated[4−6] from several cyanobacteria obtained from the LEGE-CC,[8] belonging to the species *Synechocystis salina* and also from the strain *Nodosilinea* sp. LEGE 06102. To start our search for new bartoloside producers, we used a PCR screening targeting the *brtD* and *brtB* genes, as these would be critical for the production of bartoloside and bartoloside-fatty acid ester scaffolds, respectively (Figure S1). We designed specific primers based on sequence alignments of *brtD* and *brtB* genes from previously sequenced LEGE-CC *S. salina* genomes[9] (Figure S2, Table S1). We selected 54 LEGE-CC strains (39 from the genus

Received: July 17, 2024
Revised: October 28, 2024
Accepted: October 31, 2024
Published: November 20, 2024

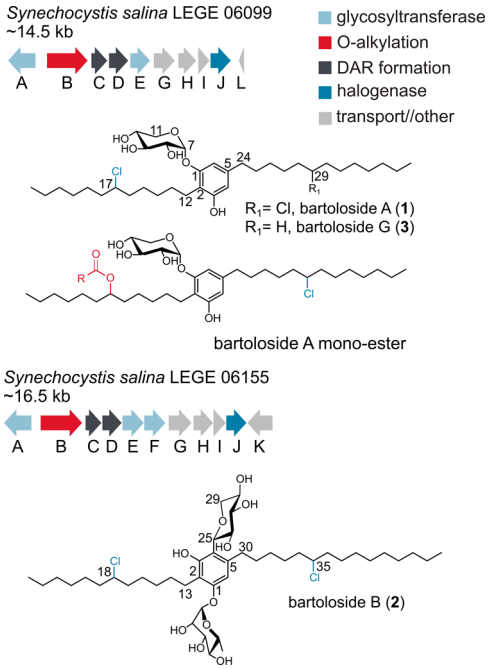

Figure 1. Overview of *brt* gene clusters from *S. salina* strains LEGE 06099 and LEGE 06155 and examples of major bartolosides previously reported from each strain.

Nodosilinea and 15 from the genus *Synechocystis*) for the PCR screening, 14 of which (three *Nodosilinea* strains and 11 *Synechocystis* strains, Figures S3−S6) led to amplification of both target genes. Most of the *Synechocystis* strains had been previously found to encode a *brtJ* homologue in a screening for dimetal-carboxylate halogenases (Figures S3−S6).[9] To detect additional bartoloside producers outside the LEGE-CC, we performed BLASTp searches for BrtB homologues and found that *Synechocystis* sp. PCC 7338 contains the *brt* BGC in its genome (Figure S7). This strain, isolated at Bodega Head (California, USA), is the first strain found to carry a *brt* BGC that does not originate from the Portuguese coast.

Because only three out of 39 *Nodosilinea* strains led to amplification of *brtB* and *brtD*, we hypothesized that the designed primers could be biased toward *Synechocystis*, given the lack of *Nodosilinea* sequence representation for primer design (Figure S2). To address this issue, we sequenced the genomes of the three *Nodosilinea* strains for which amplicons of the expected size for *brtB* and *brtD* were observed (*Nodosilinea* sp. LEGE 06191, *Nodosilinea* sp. LEGE 06069, and *Nodosilinea* sp. LEGE 07298) as well as the reported[5] bartoloside-producer *Nodosilinea* sp. LEGE 06102. However, we were not able to detect the *brt* cluster, nor any individual *brt* gene, in the resulting genome data, even though the 16S rRNA gene was consistent with the strain identities. Organic extraction followed by LC-HRESIMS analysis of these four *Nodosilinea* strains did not show the presence of bartolosides.

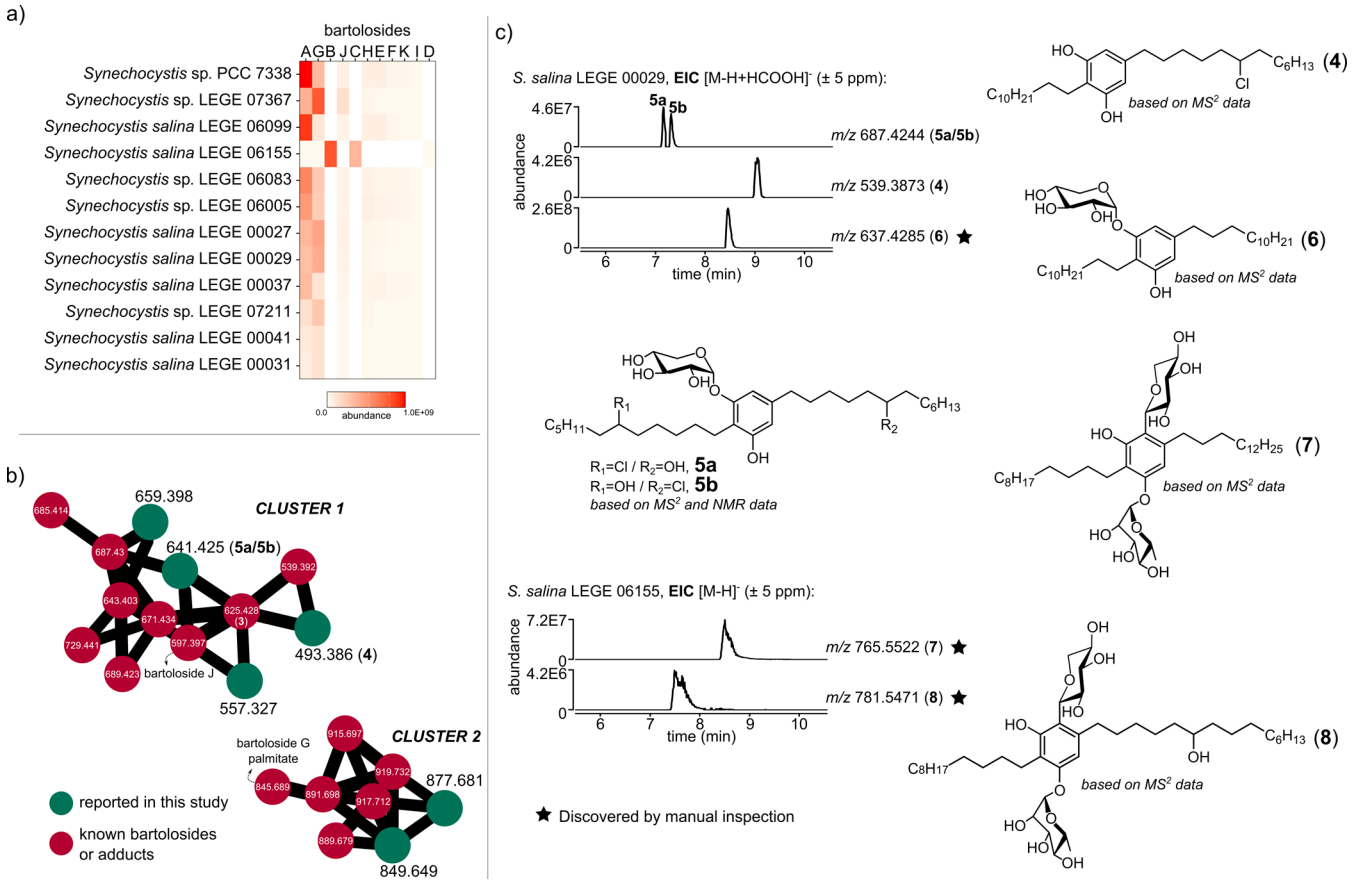

Figure 2. Detection of known and unknown bartolosides. Abundance of known bartolosides in the detected cyanobacterial producers, obtained from the area of extracted ion chromatograms (EIC) peaks obtained using LC-HRESIMS analysis and assuming similar ionization behavior (a). GNPS clusters with *m/z* were identified as new bartoloside derivatives reported in this study (b). EIC and structures of detected metabolites via GNPS and/or manual inspection (c).

https://doi.org/10.1021/acs.jnatprod.4c00832
J. Nat. Prod. 2024, 87, 2709−2715

Taking into account the low bartoloside levels reported by Leao et al.[5] for *Nodosilinea* sp. LEGE 06102 and the evidence herein gathered, we consider that the large-scale culture used for extraction and isolation in that study was likely cross-contaminated with a bartoloside-producing strain. We speculate that the DNA aliquot of the three PCR-positive *Nodosilinea* strains used was also cross-contaminated, as we could not observe possible hybridizing sequences in the sequenced genomes that could explain the amplicons observed. Hence, the *brt* BGC has, so far, been detected only in *Synechocystis* strains.

To avoid redundancy, we analyzed the 16S rRNA gene of the 11 *Synechocystis* strains obtained from the PCR screening and ruled out the ones sharing >99.85% similarity (*S. salina* LEGE 00036 and 00038 and *Synechocystis* sp. LEGE 07073; Figure S8), affording eight *Synechocystis* strains for downstream studies.

Detection of Known Bartolosides in *brt* BGC-Containing Strains. We set out to obtain metabolomic evidence of the production of bartolosides from the eight *Synechocystis* strains selected from our screening. We also included the five LEGE-CC strains (*S. salina* LEGE 00031, 00041, 06099, and 06155 and *Synechocystis* sp. 06083) known to encode the *brt* BGC (Figure S9) as well as *Synechocystis* sp. PCC 7338 (Figure S7). We analyzed the LC-HRESIMS and MS^2 data of CH_2Cl_2/MeOH (2:1, v/v) of their respective organic extracts. We could not detect any known bartoloside m/z in the extracts of *S. salina* LEGE 00030 and LEGE 00032. Although we do not have genome data for these strains, the detection of *brtJ* in a previous report[9] is consistent with the presence of the *brt* cluster, which we consider may be silent or expressed at low levels. For the remaining *Synechocystis* strains, the presence of known members of the bartoloside family was validated via comparison of their MS^2 fragmentation patterns to the literature (Figures S10−S11).[4−6] Bartoloside A (**1**) and bartoloside G (**3**) were consistently the most produced monoglycosylated bartolosides within all tested strains, with the exception of *S. salina* LEGE 06155, for which trace amounts were detected for the first time (Figure 2a, Figure S10). Considering the high natural abundance of palmitic acid in cyanobacteria,[10,11] bartoloside A-palmitate and bartoloside G-palmitate were expectedly the most abundant among the esterified bartolosides (Figure S10). LC-HRESIMS analysis of *Synechocystis* sp. PCC 7338 indicated a similar bartoloside profile compared with most LEGE-CC strains (Figure 2a), despite the geographical distance of their isolation spots (Figure S12). Diglycosylated bartolosides could only be detected in *S. salina* LEGE 06155, and bartoloside B (**2**) was found to be the most abundant derivative, as previously reported by Leao et al.[5] (Figure S11). As was the case for monoglycosylated bartoloside producing strains, we detected naturally occurring formic and palmitic acid esterified versions of bartolosides B and C in the organic extract of *S. salina* LEGE 06155 (Figure S13). These observations indicate that BrtB also accepts diglycosylated bartolosides as electrophile.[6] Although *S. salina* LEGE 06155 is the only known diglycosylated bartoloside producer, we hypothesize that *Synechocystis* sp. LEGE 07073 could also be responsible for the production of these metabolites, given the high similarity of the 16S rRNA gene (Figure S8) and the results observed in the PCR screening (Figures S3−S6).

To correlate the differences in glycosylation level and enzymatic function in the *brt* BGCs, we sequenced the genomes of the resulting six LEGE-CC *Synechocystis* strains to which bartoloside production was observed. Despite being phylogenetically close, strains producing monoglycosylated bartolosides were found to always encode two predicted glycosyltransferases (*brtA* and *brtE*) while *S. salina* LEGE 06155 encodes an additional predicted glycosyltransferase (*brtF*) (Figures S9 and S14). Hence, the initial insights into bartoloside glycosylation[4−6] remain unaltered, and the reason behind the presence, in *brt* BGCs, of one more glycosyltransferase than the number of glycosylations found in the corresponding products is unclear at this stage.

Detection of New Bartoloside Derivatives. To investigate whether additional bartolosides are produced by *brt*-containing *Synechocystis* strains, we submitted the corresponding organic extract LC-HRESIMS^2 data to the Global Natural Products Social Molecular Networking (GNPS).[7] To aid in discerning clusters of putative bartolosides, we supplied the network with data from three strains that do not produce bartolosides (*S. salina* LEGE 00032, *Nodosilinea* sp. LEGE 06069 and LEGE 07298; Figure S15). Taking into account the favored bartoloside and bartoloside ester fragmentations,[4−6] namely, the loss of glycosyl, chlorine, and/or ester moieties (Figures S10−S11), we adjusted the Minimum Matched Fragment Ion setting to "2", allowing for less-stringent metabolite clustering. Analysis of the GNPS-generated molecular network revealed the presence of a series of unknown compounds in the same cluster as bartoloside G (**3**) and bartoloside J (cluster 1, Figure 2b, Figure S15). Within this cluster, we identified a mass feature m/z 493.386 $[M-H]^-$ (**4**) with predicted molecular formula $C_{31}H_{54}ClO_2$ (calcd for m/z 493.3818 $[M-H]^-$, average experimental m/z from EIC 493.3834 $[M-H]^-$) and LC-HRESIMS^2 data consistent with a nonglycosylated bartoloside (Figure 2b,c, Figure S16). Also present in cluster 1 were two mass features with m/z 641.425 $[M-H]^-$ (representative of two putative isomers **5a**/**5b**) with the predicted molecular formula $C_{36}H_{62}ClO_7$ (calcd for m/z 641.4190 $[M-H]^-$, average experimental m/z from EIC 641.4216 $[M-H]^-$), hinting at the loss of a chlorine and gain of a hydroxy group in **1** (Figure 2b,c; Figure S16). Fragmentation of this mass feature showed the presence of a m/z 473.4018 $[M-H]^-$, also present in the reported bartoloside-ester fragmentation,[6] suggesting a midchain hydroxylation, which could result from hydrolysis of a bartoloside A fatty acid monoester species (Figure S16). Within this cluster, we identified two additional mass features with m/z 557.3275 $[M-H]^-$ and m/z 659.3984 $[M-H+HCOOH]^-$ consistent with molecular formulas $C_{30}H_{50}ClO_7$ and $C_{35}H_{60}ClO_9$, respectively (Figure 2b). The corresponding HRESIMS^2 data suggested bartoloside-like backbones modified with a hydroxy moiety as proposed for m/z 641.4216 $[M-H]^-$ (**5a**/**5b**, Figure S16).

Further analysis of a bartoloside ester-containing cluster (cluster 2) revealed two metabolites with m/z values of 849.6496 $[M-H+HCOOH]^-$ and 877.6813 $[M-H+HCOOH]^-$, consistent with formic acid adducts of bartoloside G (**3**) esterified with tridecylic and pentadecylic acids, respectively (Figure 2b, Figure S17). The presence of low levels of odd chain fatty acids in cyanobacteria has been reported;[12] hence, their esterification with bartolosides could be expected.[6]

We decided to look for additional metabolites in organic extracts and chromatographic fractions from previous isolation work with bartoloside producers.[6] Manual inspection of the

https://doi.org/10.1021/acs.jnatprod.4c00832
J. Nat. Prod. 2024, 87, 2709−2715

corresponding LC-HRESIMS data revealed a series of new metabolites with mass defects and predicted molecular formulas consistent with bartolosides. We detected several nonchlorinated derivatives of bartolosides, the most abundant being a nonchlorinated version of bartoloside A, which we named dechlorobartoloside A (**6**) with a predicted molecular formula of $C_{36}H_{63}O_6$ (calcd for m/z 591.4630 $[M-H]^-$, Figure 2c, Figures S18–S19). Additionally, other detected metabolites were also consistent with hydroxylated versions of bartolosides, as corroborated by the LC-HRESIMS^2 data, in accordance with what was reported above for **5a**/**5b** (Figure S20). The GNPS network showed that the majority of these bartoloside metabolites detected by manual inspection were clustered (cluster 3, Figure S15).

We also delved into the *S. salina* LEGE 06155 metabolome for additional bartolosides or bartoloside esters because this is the only strain reported to date as a producer of diglycosylated bartolosides. Manual inspection of the LC-HRESIMS^2 data of semipreparative HPLC fractions and organic extracts of this strain revealed six additional diglycosylated bartolosides with varying chain lengths and chlorination levels (Figure 2c, Figures S21–S22). We detected what are likely two additional hydroxylated versions of diglycosylated bartolosides based on predicted molecular formulas and LC-HRESIMS^2 data (Figure 2c, Figure S23). Dechlorobartoloside B (**7**, $C_{44}H_{77}O_{10}$ calcd for m/z 765.5522 $[M-H]^-$) and the putatively hydroxylated derivative (**8**, $C_{44}H_{77}O_{11}$ calcd for m/z 781.5471 $[M-H]^-$) were among the most abundant metabolites found. After confirming the presence of most of these metabolites in the organic extracts, we reasoned that our GNPS molecular network should have succeeded in clustering diglycosylated bartolosides as well. In fact, we found a cluster of masses exclusively produced by *S. salina* LEGE 06155 (cluster 4) connecting some of the novel diglycosylated derivatives with previously known bartolosides B (**2**) and C (Figure S15).

Isolation and Structure Elucidation of 5a/5b. To determine the structure of compounds **5a** and **5b** (m/z 641.4216 $[M-H]^-$), we carried out their isolation from a previous fraction of *S. salina* LEGE 06099 (F21) via RP-semipreparative HPLC, yielding the pure (>95%, ^{1}H NMR) subfractions F21.1 (t_R = 17.0–18.5 min, 0.8 mg, **5a**) and F21.2 (t_R = 20.2–21.8 min, 0.8 mg, **5b**). Combined HRESIMS^2 and 1D- and 2D-NMR analyses were used for the structure elucidation of **5b** (Figure 3, Figures S24–S29, Table S2) and compared to reported data for other bartolosides (Figures S29 and S30). Overall, the NMR data for **5b** were very similar to those of **1** (Figure S30, Table S2), as expected, and no differences were found for the xylose-modified resorcinol moiety, which we propose is as found in **1**.[5] Still, inspection of the ^{13}C NMR data showed the presence of a signal consistent with a tertiary carbon (CH-17, δ_C 72.4, δ_H 3.60) not present in previously reported **1**.[5] This position was COSY-correlated to two methylenes (CH_2-16/18, δ_C 37.7, δ_H 1.43 and CH_2-16/18, δ_C 37.4, δ_H 1.43). The absence of significant differences in the ^{1}H and ^{13}C resonances of the aromatic ring and xylose moiety pointed toward the hydroxylation occurring in one of the alkyl chains of the DAR moiety, as speculated above. The chlorinated position and its vicinal methylenes did not show discernible differences compared with the reported data[5] for **1**, suggesting that hydroxylation was located in the non-chlorinated alkyl chain. This was confirmed by HRESIMS^2 analysis of an *in-source* generated fragment of **5b** (m/z 473.4000 $[M-H]^-$, corresponding to the loss of glycosyl and

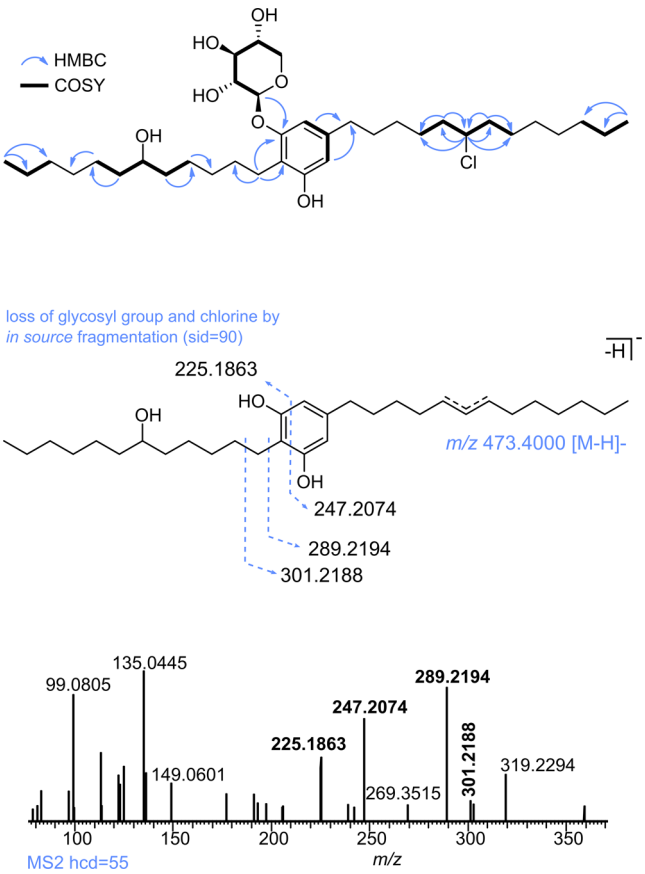

Figure 3. Structure elucidation of compound **5b**. Depicted are the NMR (COSY and HMBC) correlations observed and the HRESIMS^2 data of *in-source* generated fragment m/z 473.4000 $[M-H]^-$ for hydroxylated chain assignment.

chlorine moieties, Figure 3). The positioning of the hydroxy group is proposed to correspond to the chlorinated position in **1**, based on the correlational data and because the resonances of the adjacent positions are consistent with the NMR data for this compound (Figure 3, Figures S29–S30). ^{1}H and ^{13}C NMR and LC-HRESIMS^2 analysis of **5a** confirmed its structural isomerism to **5b** (Figures S16, Figures S31–S32, Table S3). Fragmentation of the *in-source* generated fragment m/z 473.4000 $[M-H]^-$ was used to assign the hydroxylation of **5a** to the C-5 alkyl chain (Figure S33). With this, we were able to determine the hydroxylated alkyl chain in most of the additional hydroxylated bartolosides derivatives detected in this study (Table S4), through comparison of fragmentation patterns of parent ions and their corresponding *in-source* generated fragments MS^2. We propose that the positioning of the hydroxy groups, as for **5b**, corresponds to the same positions that are halogenated in the corresponding chlorinated bartolosides of equal alkyl chain size. The absolute configurations of **5a**/**5b** were not established given the isolated positioning of the stereocenters in the alkyl chains and the previous lack of success in crystallization of pure bartolosides.[4,5]

The discovery of minute amounts of hydroxylated bartolosides herein is intriguing. Given the positioning of the hydroxylation in **5b**, the same position that is chlorinated in **1** and eventually is converted to an esterified position by BrtB, it is possible that such hydroxylations are the result of bartoloside ester hydrolysis. On the other hand, while all other

https://doi.org/10.1021/acs.jnatprod.4c00832
J. Nat. Prod. 2024, 87, 2709–2715

enzmes in the *brt* BGC are assigned to a biosynthetic function,[4−6] it cannot be ruled out that the halogenase BrtJ itself can perform hydroxylation. Both nonheme iron/2-oxoglutarate-dependent and flavin-dependent halogenases[9] trace back to oxygenases[13,14] and, for example, a single mutation in the *Burkholderia ambifaria* SadA hydroxylase turns it into an halogenase.[15] Previous bioinformatic studies have shown that BrtJ belongs to a new family of dimetal halogenases typified by CylC, the halogenase involved in the biosynthesis of cylindrocyclophanes, but for which we lack mechanistic details.[9,16] Other putative halogenases from this family have already been associated with the production of other chlorinated cyanobacterial metabolites, e.g., NglC involved in the biosynthesis of nostochlorosides.[17] Hydroxylated versions of the chlorinated metabolites associated with CylC homologues[16,17] have not been reported.

CONCLUSION

This work has led to the discovery of several new bartolosides and bartoloside esters, expanding the structural diversity of this natural product family and highlighting the substrate promiscuity associated with its biosynthetic pathway. The presence of a *brt* cluster in *Synechocystis* sp. PCC 7338, isolated from a distant location from all of the other reported *brt*-containing cyanobacteria, suggests that these metabolites might be geographically disperse. Metabolic profiling of the detected bartoloside-producing strains showed homogeneity in terms of bartoloside abundance and distribution (with the exception of the diglycosylated bartoloside producer), further supporting a fundamental role for these metabolites in certain *Synechocystis* cyanobacteria. The biosynthetic basis for the novel hydroxylated bartolosides remains to be elucidated and could be the result of bartoloside-ester hydrolysis (e.g., to recycle fatty acids) or of a previously unrecognized ability of dimetal carboxylate halogenases to perform oxygenation.

EXPERIMENTAL SECTION

General Experimental Procedures. Optical rotations were measured in a Jasco P-2000 polarimeter controlled by the SpectraManager 2.14.02 software. UV spectra were acquired on a UV-1600PC spectrometer controlled by MWAVE v.1.0.20 software (VWR). Infrared spectra were acquired in a Nicolet iS5 FTIR spectrometer controlled by OMNIC 9.8.372 software (ThermoScientific). One- and two-dimensional NMR spectra were obtained in the Materials Center of the University of Porto (CEMUP) on a Bruker Avance III, 400 MHz instrument controlled by TopSpin 3.2. Chemical shifts are reported in parts per million (ppm) and using the residual solvent resonances as reference for ^{1}H ($CDCl_3$, 7.26 ppm) and ^{13}C ($CDCl_3$, 77.16 ppm). NMR data was analyzed in MNova 12.0.4.

LC-HRESIMS and LC-HRESIMS/MS (HCD, Higher energy collisional dissociation) analyses were performed on an UltiMate 3000 UHPLC (Thermo Fisher Scientific) system composed of a LPG-3400SD pump, WPS-3000SL autosampler, and VWD-3100 UV/vis detector coupled to a Q Exactive Focus Hybrid Quadrupole-Orbitrap Mass Spectrometer controlled by Q Exactive Focus Tune 2.9 and Xcalibur 4.1 (Thermo Fisher Scientific). LC-HRESIMS data was obtained in Full Scan mode, with a capillary voltage of HESI set to −3.8 kV and the capillary temperature set to 300 °C. Sheath gas flow rate was set to 35 units.

LC-MS solvents were obtained from Thermo Fisher Scientific, Fluka, and Carlo Erba. All solvents were ACS grade except for HPLC solvents (HPLC gradient grade) and LC-MS solvents (MS-grade). Deuterated solvents for NMR were acquired from Eurisotop (Cambridge Isotope Laboratories).

Oligonucleotides were synthesized by Eurofins Genomics. PCR reactions were carried out in a Veriti 96-well thermal cycler (Applied Biosystems) and using the NZY*Taq*II Supreme Mix (NZYTech). Genomic DNA sequencing was performed by Microbial Genomics Ltd.

Phylogenetic Analysis. Nucleotide sequences of the available 16S data from bartoloside producers were aligned using MUSCLE, from within Geneious Prime 2024.0.5 (Biomatters). The resulting alignment (with a total of 57 sequences) was trimmed to its core region and contained 599 positions. FastTree 2.1.11[18] (from within Geneious Prime 2024.0.5) was used to compute an approximately maximum-likelihood phylogenetic tree, using pseudocounts and 100 rate categories of sites.

Primer Design and PCR Screening. Available nucleotide sequences of *brtB* and *brtD* from previously sequenced *brt*-containing strains (*S. salina* LEGE 06099, LEGE 00031, LEGE 00041, LEGE 06083, and LEGE 06155) were aligned using MUSCLE from within Geneious Prime 2024.0.5 (Biomatters). For the primer design, we considered highly conserved regions and only substituted 2 nucleotides in the forward primer for *brtD* amplification as shown in Figure S2 and Table S1.

Genomic DNA was obtained from dilution of stocks from the LEGE-CC[8] to a concentration of 5 ng·μL and was used for the PCR amplification of *brtB* and *brtD*. The reaction was prepared in a volume of 12.5 μL, containing 1xNZY*Taq*II Supreme Mix, 0.5 μM of each primer, and 1 μL of template gDNA. The PCR cycling program consisted of an initial denaturation at 95 °C followed by 35 cycles of denaturation at 94 °C for 30 s, 56/58 °C (*brtB*/*brtD*) for 30 s, extension at 72 °C for 30 s, and final extension at 72 °C for 7 min.

Culture Conditions. Cyanobacteria used in this work were obtained from the LEGE-CC[8] and PCC culture collections. Cultures were grown in Z8 medium or Z8 medium supplemented with 25 g·L^{-1} sea salt (Tropic Marin), at 25 °C, under a 14:10 h light/dark cycle and constant aeration. Cyanobacteria were cultured in 50 mL plastic flasks, and cells were harvested after 15 days by centrifugation at 4500*g*, 10 min, 4 °C, rinsed with deionized H_2O, and centrifuged again. The resulting biomass pellets were extracted with CH_2Cl_2/MeOH (2:1, v/v) at room temperature. Organic extracts were analyzed by LC-HRESIMS.

LC-HRESIMS Analysis. For LC-HRESIMS organic extract analyses, separation was performed on an ACE Ultracore Super C18 column (75 × 2.1 mm, 2.5 μm, 95 Å, ACE). Mixtures of MeOH/H_2O 1:1 (v/v) with 0.1% formic acid (eluent A) and IPA with 0.1% formic acid (eluent B) were used as mobile phase, with a flow rate of 0.4 mL·min^{-1}. Organic extracts were separated (4 μL of a 2 mg·mL^{-1} solution were injected) using a gradient of 10% B during 1 min, increased to 65% B over 5 min and held for 12 min, and then increased to 85% B over 2 min and held for 9 min before returning to the initial conditions.

For LC-HRESIMS analyses, fractions obtained from previous work with bartolosides[6] were analyzed (4 μL at 0.5 mg mL^{-1} per injection) in a Luna C18 column (100 × 3 mm, 3 μm, 100 Å, Phenomenex). The separation used a gradient of 10% B increasing to 70% B over 10 min and was held for 7 min prior to returning to the initial conditions. LC-HRESIMS analyses of semipreparative HPLC subfractions of *S. salina* LEGE 06155 were performed in an ACE Ultracore Super C18 column (75 × 2.1 mm, 2.5 μm, 95 Å, ACE), and the compounds were separated (4 μL of a 0.1 to 0.5 mg·mL^{-1} solution were injected) using a gradient of 10% B during 1 min, increased to 85% B over 7 min, and held for 10 min before returning to the initial conditions. LC-HRESIMS of **5a** and **5b** for $ddMS^2$ of dialkylresorcinol moiety was performed using an ACE Ultracore Super C18 column (75 × 2.1 mm, 2.5 μm, 95 Å, ACE), and compounds were separated (4 μL of a 0.1 mg·mL^{-1} solution were injected) using a gradient of 10% B during 1 min, increased to 65% B over 11 min, and then returned to the initial conditions.

MS/MS Analysis. MS/MS parameters for the LC-HRESIMS/MS analysis of organic extracts were as follows: fractions from Reis et al.[6] and fractions from work with *S. salina* LEGE 06155 had a resolution of 35 000, with a 1 *m*/*z* isolation window, a loop count of 3, AGC

https://doi.org/10.1021/acs.jnatprod.4c00832
J. Nat. Prod. 2024, 87, 2709−2715

target of 5×10^4, and collision energy of 35, 45, and/or 60 eV depending on the molecule.

To obtain structural information regarding the dialkylresorcinol moiety, isolation of *in-source*-formed species was selected for $ddMS^2$ events.[4,6] The *in-source* collision induced dissociation (CID) energy was set to 80/90 eV (to isolate species corresponding to the loss of glycosyl and chlorine moieties as shown in the Supporting Information), resolution of 35 000, loop count of 3, AGC target of 5×10^4, and with 1 or 2 m/z isolation window, for monoglycosylated and diglycosylated bartolosides, respectively. CID energy was set to 35 or 55 eV for monoglycosylated bartolosides and 60 eV for diglycosylated derivatives. For purified compounds **5a** and **5b**, this analysis was performed using a collision energy of 55 eV.

Molecular Networking. LC-HRESIMS/MS raw data files of each tested bartoloside producer and selected nonproducers (*S. salina* LEGE 00032, *Nodosilinea* sp. LEGE 06069 and LEGE 07298) and also the blanks of the run were converted to the mzML format using MSConvert, using the parameters recommended for GNPS molecular networking. The appropriate files were uploaded to the GNPS web platform using the default parameters recommended for high-resolution MS data except the Minimum Matched Ion Fragment, which was set to "2". The molecular network was created using feature-based molecular networking analysis on GNPS and visualized in Cytoscape 3.10.1. The m/z values retrieved from GNPS were used to search the organic extracts LC-HRESIMS data, and the average experimental m/z from the corresponding EICs was determined and used to derive molecular formulas.

Isolation of Hydroxylated Bartolosides 5a and 5b. After observing the presence of the desired compounds **5a** and **5b** in a previous fraction of *S. salina* LEGE 06099,[6] we proceeded with the isolation via reversed-phase semipreparative HPLC. The separation was performed in an ACE C18 column (100 Å pore size, 250 × 10 mm, 5 μm, ACE) using mobile phase A (H_2O), B (MeCN), and C (IPA) with a flow rate of 3 mL·min^{-1}. The LC method started with an isocratic step of 20% A, 80% B for 30 min, increased to 100% B over 3 min, and then swapped to 70% B, 30% C over 5 min, held for 10 min, and went back to 100% B over 3 min prior to returning to the initial conditions. This procedure afforded 7 subfractions. Fractions F21.1 (compound **5a**, 0.8 mg, t_R = 17.0−18.5 min) and F21.2 (compound **5b**, 0.8 mg, t_R = 20.2−21.8 min) were spectroscopically pure, showing signals characteristic of bartolosides.[4−6]

*29-Dechloro-29-hydroxybartoloside A (**5a**).* White-transparent, glassy solid; $[\alpha]^{25}_D$ −3.0 (*c* 0.60, MeOH); UV (MeOH) λ_{max} (log ε) 228 (3.3), 232 (3.3), 273 (3.0), 395 (2.0); IR (thin film) υ_{max} 2969, 2945, 2867, 2364, 2345, 1872, 1847, 1835, 1656, 1562, 1545, 1526, 1462, 1424 cm^{-1}; ^{1}H and ^{13}C NMR data, Table S3; HRESIMS m/z 641.4216 $[M-H]^-$ (calcd for $C_{36}H_{62}ClO_7$, m/z 641.4190 $[M-H]^-$).

*17-Dechloro-17-hydroxybartoloside A (**5b**).* White-transparent, glassy solid; $[\alpha]^{25}_D$ −6.0 (*c* 0.65, MeOH); UV (MeOH) λ_{max} (log ε) 228 (3.3), 231 (3.3), 273 (3.0), 397 (2.0); IR (thin film) υ_{max} 3856, 3752, 3002, 2978, 2962, 2930, 2890, 2852, 2839, 2365, 2347, 1871, 1847, 1833, 1795, 1777, 1656, 1563, 1544, 1525, 1510, 1461, 1421 cm^{-1}; ^{1}H and ^{13}C NMR data, Table S2; HRESIMS m/z 641.4216 $[M-H]^-$ (calcd for $C_{36}H_{62}ClO_7$, m/z 641.4190 $[M-H]^-$).

■ ASSOCIATED CONTENT

Data Availability Statement

The NMR data for **5a** and **5b** has been deposited in the Natural Products Magnetic Resonance Database (NP-MRD; www.np-mrd.org) and can be found at NP0341817 (**5a**) and NP0341815 (**5b**).

Supporting Information

The Supporting Information is available free of charge at https://pubs.acs.org/doi/10.1021/acs.jnatprod.4c00832.

NMR data for **5a** and **5b**, annotated $HRESIMS^n$ data, phylogenetic analysis of the cyanobacterium strain, details on primer design, and annotation of the *brt* gene cluster (PDF)

■ AUTHOR INFORMATION

Corresponding Author

Pedro N. Leão − *CIIMAR − Interdisciplinary Centre of Marine and Environmental Research, University of Porto, Matosinhos 4450-208, Portugal;* orcid.org/0000-0001-5064-9164; Email: pleao@ciimar.up.pt

Authors

João P. A. Reis − *CIIMAR − Interdisciplinary Centre of Marine and Environmental Research, University of Porto, Matosinhos 4450-208, Portugal; ICBAS − School of Medicine and Biomedical Sciences, University of Porto, Matosinhos 4450-208, Portugal*

Sara Freitas − *CIIMAR − Interdisciplinary Centre of Marine and Environmental Research, University of Porto, Matosinhos 4450-208, Portugal*

Tereza Procházková − *CIIMAR − Interdisciplinary Centre of Marine and Environmental Research, University of Porto, Matosinhos 4450-208, Portugal; RECETOX − Research Centre for Toxic Compounds in the Environment, Faculty of Science, Masaryk University, Brno 625 00, Czech Republic*

Complete contact information is available at: https://pubs.acs.org/10.1021/acs.jnatprod.4c00832

Funding

This work is funded by national funds through FCT (Fundação para a Ciência e a Tecnologia), within the scope of the project PTDC/BIA-BQM/5760/2020 (DOI: 10.54499/PTDC/BIA-BQM/5760/2020) and strategic funding grants UIDB/04423/2020 and UIDP/04423/2020, and through the European Union's Horizon 2020 Research and Innovation Programme (GA no. 952374). J.P.A. Reis was supported by FCT grant 2020.08337.BD.

Notes

The authors declare no competing financial interest.

■ REFERENCES

(1) Dittmann, E.; Gugger, M.; Sivonen, K.; Fewer, D. P. *Trends Microbiol* **2015**, *23* (10), 642−652.

(2) Gavriilidou, A.; Kautsar, S. A.; Zaburannyi, N.; Krug, D.; Müller, R.; Medema, M. H.; Ziemert, N. *Nat. Microbiol* **2022**, *7* (5), 726−735.

(3) Pye, C. R.; Bertin, M. J.; Lokey, R. S.; Gerwick, W. H.; Linington, R. G. *Proc. Natl. Acad. Sci. U.S.A.* **2017**, *114* (22), 5601−5606.

(4) Afonso, T. B.; Costa, M. S.; Rezende de Castro, R.; Freitas, S.; Silva, A.; Schneider, M. P.; Martins, R.; Leao, P. N. *J. Nat. Prod* **2016**, *79* (10), 2504−2513.

(5) Leao, P. N.; Nakamura, H.; Costa, M.; Pereira, A. R.; Martins, R.; Vasconcelos, V.; Gerwick, W. H.; Balskus, E. P. *Angew. Chem., Int. Ed. Engl.* **2015**, *54* (38), 11063−11067.

(6) Reis, J. P. A.; Figueiredo, S. A. C.; Sousa, M. L.; Leao, P. N. *Nat. Commun.* **2020**, *11* (1), 1458.

(7) Wang, M.; Carver, J. J.; Phelan, V. V.; Sanchez, L. M.; Garg, N.; Peng, Y.; Nguyen, D. D.; Watrous, J.; Kapono, C. A.; Luzzatto-Knaan, T.; et al. *Nat. Biotechnol.* **2016**, *34* (8), 828−837.

(8) Ramos, V.; Morais, J.; Castelo-Branco, R.; Pinheiro, Â.; Martins, J.; Regueiras, A.; Pereira, A. L.; Lopes, V. R.; Frazão, B.; Gomes, D.; et al. *J. Appl. Phycol* **2018**, *30* (3), 1437−1451.

(9) Eusébio, N.; Castelo-Branco, R.; Sousa, D.; Preto, M.; D'Agostino, P.; Gulder, T. A. M.; Leão, P. N. *ACS Synth. Biol.* **2022**, *11* (10), 3493−3503.

(10) Eungrasamee, K.; Incharoensakdi, A.; Lindblad, P.; Jantaro, S. *Sci. Rep* **2020**, *10* (1), 4515.

(11) Sallal, A. K.; Nimer, N. A.; Radwan, S. S. *Microbiol* **1990**, *136* (10), 2043−2048.

(12) Shan, Y.; Liu, Y.; Yang, L.; Nie, H.; Shen, S.; Dong, C.; Bai, Y.; Sun, Q.; Zhao, J.; Liu, H. *J. Sep Sci.* **2016**, *39* (19), 3745−3753.
(13) Menon, B. R. K.; Richmond, D.; Menon, N. *Catal. Rev.* **2022**, *64* (3), 533−591.
(14) Martinez, S.; Hausinger, R. P. *JBC* **2015**, *290* (34), 20702−20711.
(15) Mitchell, A. J.; Dunham, N. P.; Bergman, J. A.; Wang, B.; Zhu, Q.; Chang, W.-c.; Liu, X.; Boal, A. K. *Biochem* **2017**, *56* (3), 441−444.
(16) Nakamura, H.; Hamer, H. A.; Sirasani, G.; Balskus, E. P. *J. Am. Chem. Soc.* **2012**, *134* (45), 18518−18521.
(17) Glasser, N. R.; Cui, D.; Risser, D. D.; Okafor, C. D.; Balskus, E. P. *Nat. Chem.* **2024**, *16* (2), 173−182.
(18) Price, M. N.; Dehal, P. S.; Arkin, A. P. *PLoS One* **2010**, *5* (3), No. e9490.

https://doi.org/10.1021/acs.jnatprod.4c00832
J. Nat. Prod. 2024, 87, 2709−2715